JOINT INSTITUTE FOR NUCLEAR RESEARCH
Flerov Laboratory of Nuclear Reactions

FINAL REPORT ON THE START PROGRAMME

Simulation of Swift Heavy Ion Effects in α-Gallium Nitride

Supervisor:
Dr. Ruslan Alikovich Rymzhanov

Student:
Semen Moskalets, Russia
Far Eastern Federal University

Participation period:
August 24 – October 18,
Summer Session 2024

Dubna, 2024

Abstract

Swift heavy ion effects simulation in wurtzite gallium nitride structure was performed. Monte-Carlo method was used in TREKIS program to describe kinetics of the electronic subsystem and Molecular Dynamics method was used in LAMMPS program for lattice atoms kinetics description. Simulations for Pb ion with 132 MeV energy show that track formation depends on the orientation of incoming ion trajectory relative to lattice. The obtained ion tracks show that material has certain directions of weak recrystallization.

Contents

1. Introduction

Gallium nitride is a perspective material for electronics. Transistors based on gallium nitride have several features that make them a really attractive solution for use in spacecraft power systems [1]. In space materials are exposed to cosmic radiation, which leads to device malfunctions. That is why we need to know the material radiation resistivity and its other properties. Swift heavy ion (SHI) irradiation effects are in some way analogous to the cosmic rays effects, and SHI simulation may provide information about the applicability of material for space uses.

While passing through the matter, SHI lose most of their energy to excite the electronic subsystem. The thermalization time of the electronic subsystem is ~100 fs. Then the excess energy is transferred to the lattice of the material. After that processes of nuclear subsystem relaxation occur. So, the task may be divided into two parts: electronic subsystem excitation (< 100 fs) and atomic system relaxation (> 100 fs). These problems are solved by two different methods – Monte-Carlo (MC) simulation and Molecular Dynamics (MD) simulation.

The first method is applied in TREKIS program (Time Resolved Electron Kinetics in SHI Irradiated Solids) [2]. MC simulation is based on a large number of implementations of a random process (interactions in our problem). Its probability is determined from the interaction cross sections. The program traces each scattering event in detail on each iteration. The TREKIS output data are the radial density distributions of electrons and holes and their energy densities, the angular distributions of the generated electrons, and the distribution of excess energy in the lattice of the material.

The second method is applied in LAMMPS program (Large-scale Atomic/Molecular Massively Parallel Simulator) [3]. MD is an approach in which the temporal evolution of a system of interacting atoms is tracked by integrating their motion equations. The first step there is to set the positions of material atoms. Describing interatomic interaction requires interatomic potential. The LAMMPS output data are coordinates and velocities of atoms at different timesteps. This data represents time evolution of a given system and contains structural information.

2. Simulation

2.1 Construction of the energy loss function

For MC modeling of excitation of electronic subsystem by an incoming SHI, the TREKIS program requires interaction cross sections $\frac{d^2\sigma}{d(\hbar\omega)d(\hbar q)}$. The first-order Born approximation allows to express scattering cross section of a particle on a system of coupled particles as product of interaction cross section with a free scatterer and dynamic structural factor (DSF) [4] $S(\boldsymbol{q},\omega)$. And DSF is associated with a complex dielectric function $\varepsilon(\boldsymbol{q},\omega)$. This allows us to express the scattering cross section in terms of CDF:

$$\frac{d^2\sigma}{d(h\omega)\,d(hq)} = \frac{2(Z_e(v,q)e)^2}{n_{sc}\pi\hbar^2v^2}\frac{1}{hq}\,\mathrm{Im}\left(\frac{-1}{\varepsilon(\boldsymbol{q},\omega)}\right) \tag{1}$$

where $Z_e(v,q)$ – effective ion charge in medium as function of velocity v and transferred momentum q, n_{sc} – density of scatterers (electrons), and $\mathrm{Im}\left(\frac{-1}{\varepsilon(\boldsymbol{q},\omega)}\right)$ – energy loss function.

For complex systems, analytical form of loss function is unknown. Therefore, it was constructed from available experimental and calculated data. The values of complex refractive index $n^* = n + ik$ were taken from S. Adachi handbook [5]: a complete set of optical constants for phonon peak region ($0.01 - 0.5$ eV) was calculated using reststrahlen parameters of H. Sobotta *et al.* [6]; the optical constants for $3.35 - 9.55$ eV energy values were obtained by Logothetidis *et al.* [7] using ellipsometry method. The valence peak region ($4.25 - 29.5$ eV) was taken from the work of Olson *et al.* [8], where the reflectance of gallium nitride has been measured and Kramers-Kronig analyzed to get the energy loss function. For $30 - 30000$ eV energy region loss function was calculated from attenuation lengths λ_a, obtained from B.L. Henke database [9]. Based on this data, the loss function was calculated using the following formulae:

$$\mathrm{Im}\left(\frac{-1}{\varepsilon(\boldsymbol{q},\omega)}\right) = \frac{2nk}{(n^2-k^2)^2+(2nk)^2} \tag{2}$$

$$\mathrm{Im}\left(\frac{-1}{\varepsilon(\boldsymbol{q},\omega)}\right)=\frac{c}{\lambda_a\omega} \tag{3}$$

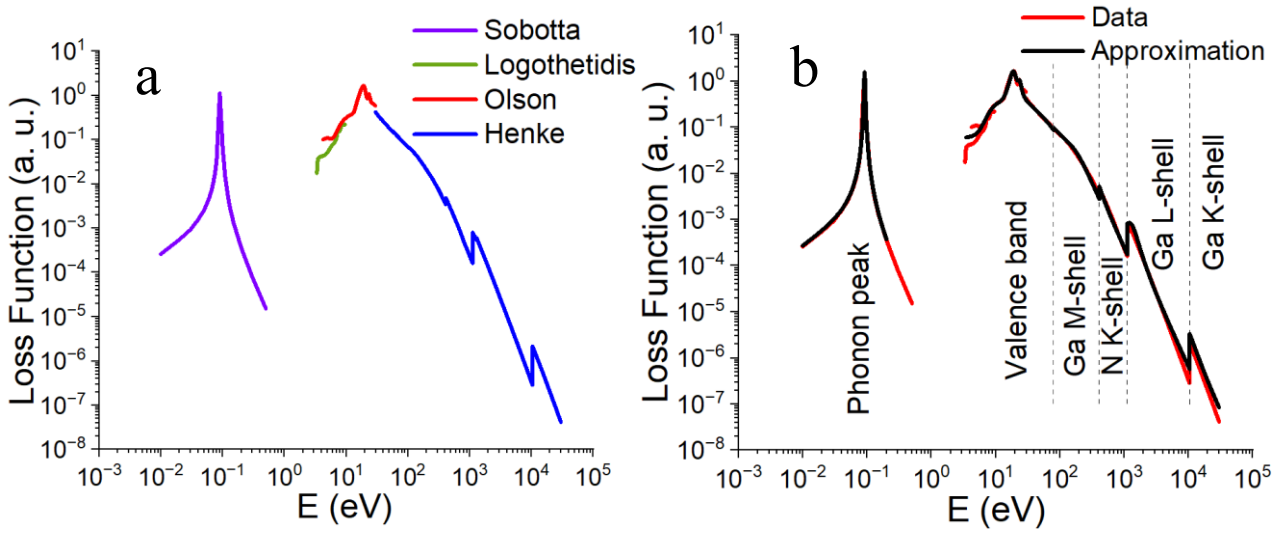

Figure 1. Energy loss function constructed from data (a), and comparison with approximation (b).

The graph of constructed loss function consists of peaks corresponding to the electronic shells of the material elements, and optical phonons peak (Fig. 1a). According to Ritchie and Howie [10] the analytical form of the loss function can be approximated with a sum of oscillator functions:

$$\mathrm{Im}\left(\frac{-1}{\varepsilon(\boldsymbol{q},\omega)}\right)=\sum_i \frac{A_i\gamma_i\hbar\omega}{(\hbar^2\omega^2-E_{0i}^2)^2+(\gamma_i\hbar\omega)^2} \tag{4}$$

where A_i, E_{0i}, γ_i – parameters, corresponding to amplitude, position, and width of i-th oscillator respectively. They have been determined by a fitting procedure of the optical data (Table 1), so that the analytical and experimental curves matched as much as possible (Fig. 1b).

Table 1. Fitting parameters and sum rules test results.

	E_{0i}	A_i	γ_i	KK-sum	f-sum (N_e)
Valence band	35.3	977	101	0.78504	17.97781 (18)
	18.9	116	5		
	23.7	24	3.24		
	13.8	-18.7	7.7		
	7	-11.6	8		
Ga M-shell	164	55	180	0.01202	8.03395 (8)
N K-shell	320	316	150	0.00032	1.93287 (2)
Ga L-shell	1270	600	680	0.00018	7.95068 (8)
Ga K-shell	8600	230	6300	0	2.01809 (2)
Phonon peak	9.16E-2	5.17E-4	3.64E-3	0.061445	--

Total:		0.859005 (1)	37.9134 (38)

Then the obtained loss function was tested to satisfy the f-sum and KK-sum rules [11] [12], given by formulae:

$$\frac{2}{\pi\Omega_P^2}\int_0^{\hbar\omega_{i\,max}} \mathrm{Im}\left(\frac{-1}{\varepsilon(\boldsymbol{q},\omega)}\right)\hbar\omega\; d(\hbar\omega) = N_{ei} \tag{5}$$

$$\frac{2}{\pi}\int_0^{\infty} \mathrm{Im}\left(\frac{-1}{\varepsilon(\boldsymbol{q},\omega)}\right)\frac{d(\hbar\omega)}{\hbar\omega} = 1 \tag{6}$$

where index i corresponds to atomic shell, Ω_P is plasma frequency, N_{ei} is number of electrons of a given shell. The testing results (Table 1) indicate a reliable determination of the loss function analytical form (here gallium 3d-subshell is included to the valence peak region).

And lastly, SHI energy losses, computed by TREKIS pre-MC calculations, were compared with corresponding computation results of SRIM program [13]. The comparison was carried out for ions of different charges (Ne, Xe, Kr, Au). The data from these programs are in good agreement, the heights of the Bragg peak differ by less than 10% (Fig. 2). After energy loss function validation, Monte-Carlo calculations can be performed.

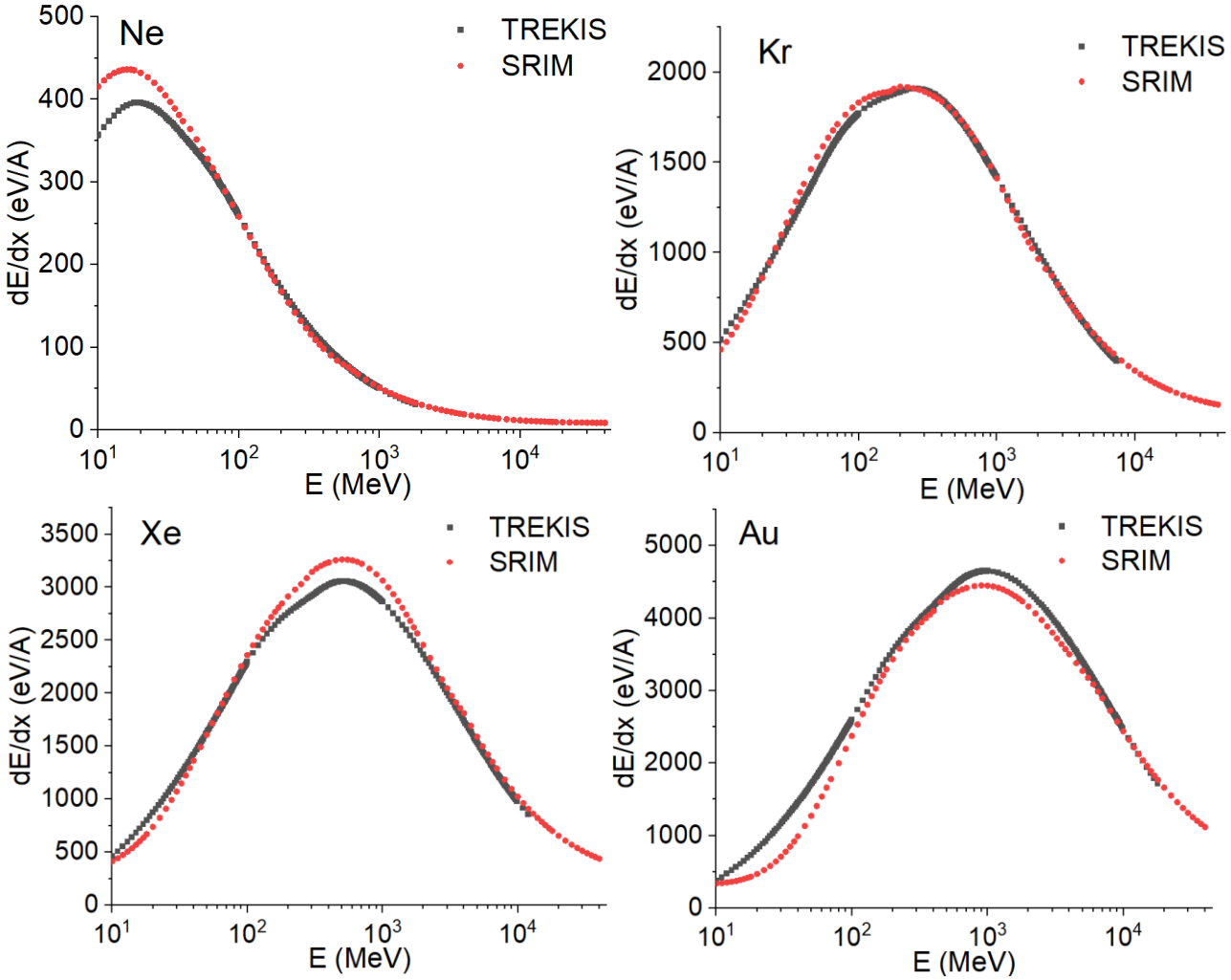

Figure 2. Dependence of ionization losses of Ne, Kr, Xe, Au ions on the energy of the incoming particle.

2.2 Monte-Carlo simulation

The constructed energy loss function was used to calculate the differential interaction cross sections according to formula (1). These cross sections were used by TREKIS program for Monte-Carlo event-by-event simulation of SHI passage through material. The trajectory of the incoming ion was chosen perpendicular to the surface of the material. It is assumed that the ion loses energy only to excite the electronic subsystem. Simulation starts from the moment of ion passing through and ends after 100 fs. Each such simulation corresponds to one iteration of MC calculation.

In this work MC calculations were performed with 1000 iterations for Pb ion with 132 MeV energy. The choice of ion and energy was dictated by availability of experimental data in literature [14]. As a result, radial energy density distributions for electrons, holes, and lattice were obtained at different stages of the simulation (Fig. 3).

The final lattice energy density distribution (100 fs) was then used to determine velocity distribution for molecular dynamics calculations.

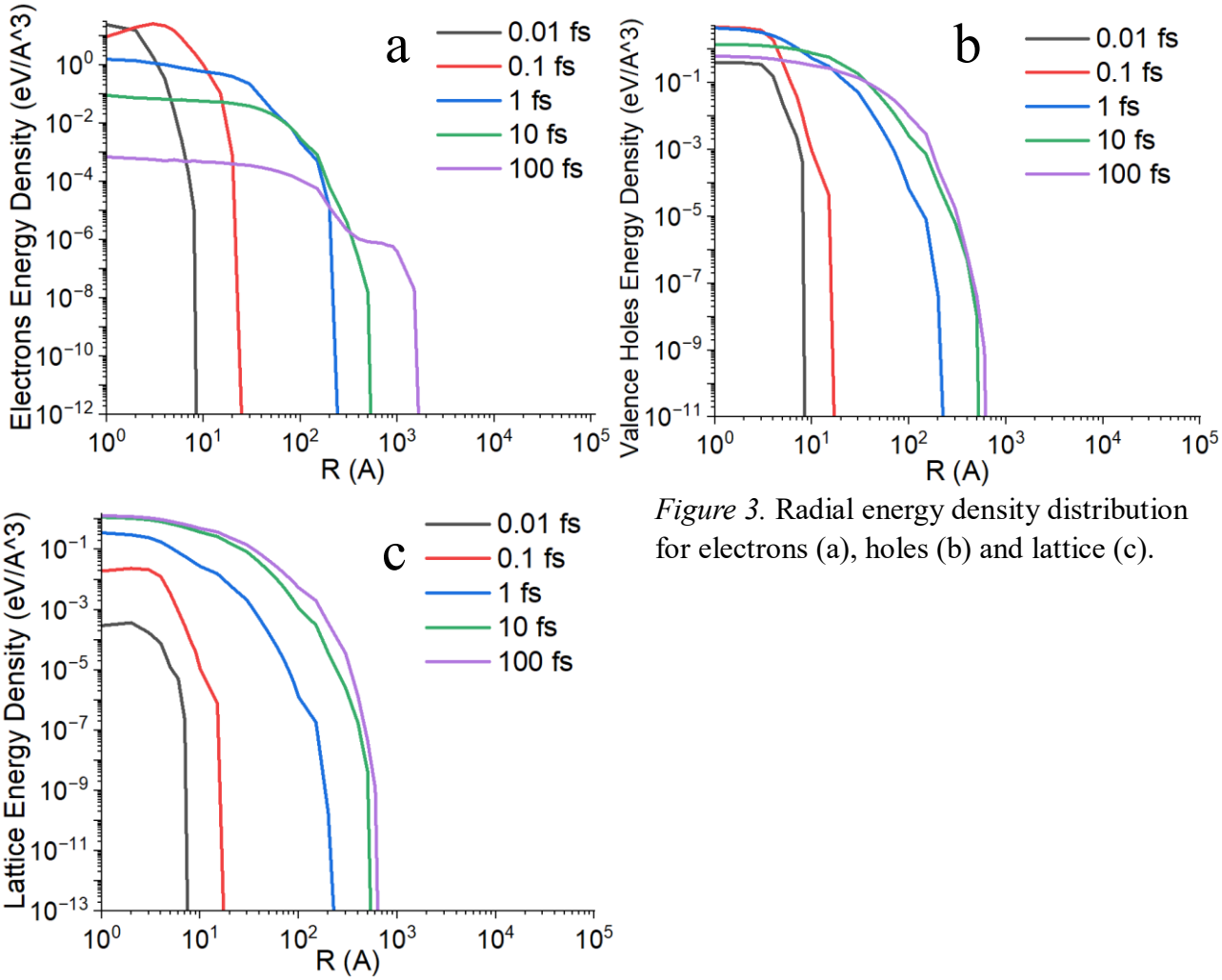

Figure 3. Radial energy density distribution for electrons (a), holes (b) and lattice (c).

2.3 Molecular dynamics simulation

Molecular dynamics calculations were performed in LAMMPS program for α-GaN crystal (Fig. 4). The program simulates temporal evolution of a system of interacting particles by integrating their motion equations. To do this, it is necessary to set the interatomic potential for gallium nitride crystal.

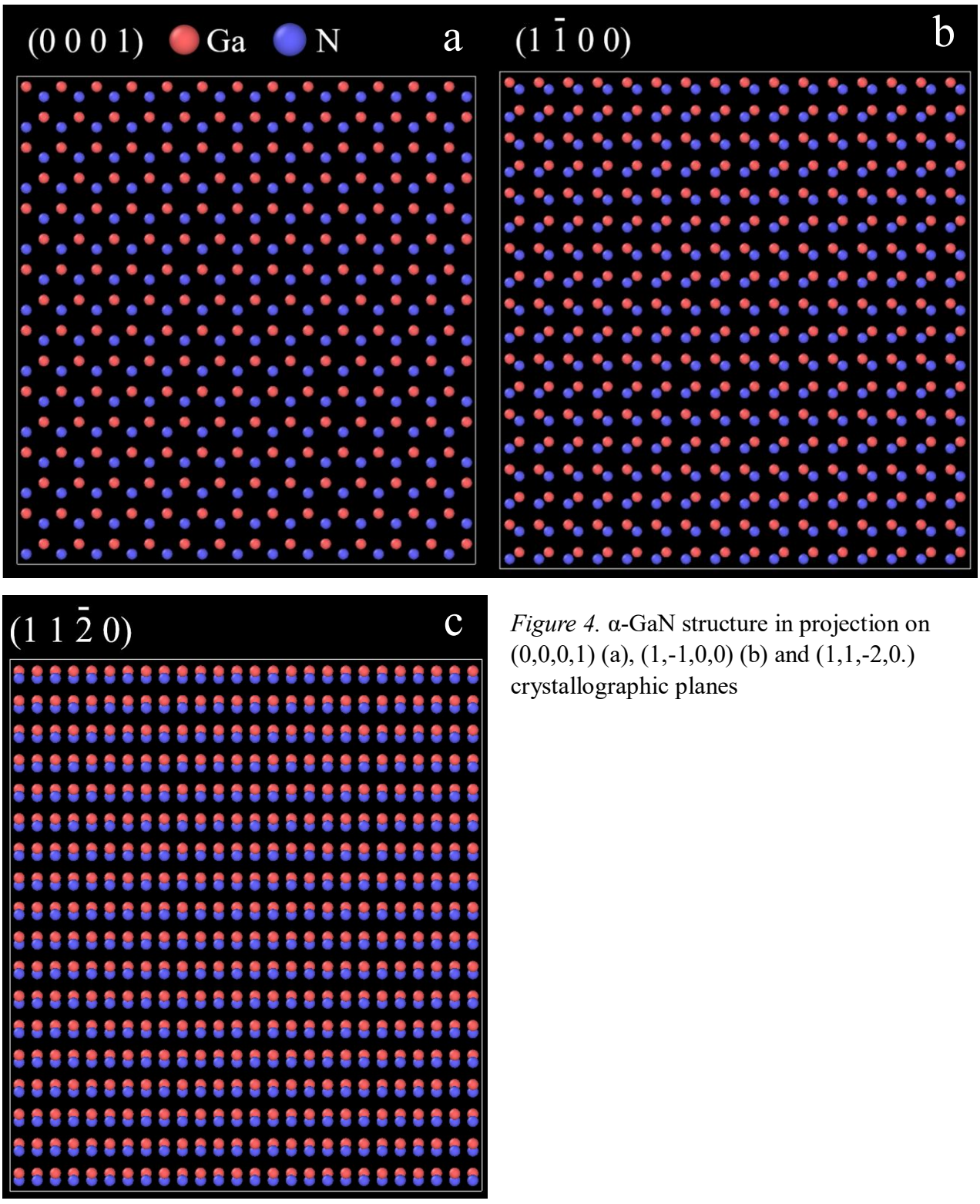

Figure 4. α-GaN structure in projection on (0,0,0,1) (a), (1,-1,0,0) (b) and (1,1,-2,0.) crystallographic planes

J. Nord *et al.* [15] presented the Tersoff-Brenner potential, describing a wide range of structural properties of gallium nitride: point defect formation energies, melting point, solubility of nitrogen atoms in liquid gallium.

A. Bere and A. Serra [16] adapted the empirical Stillinger-Weber potential to describe interatomic interactions in gallium nitride. The potential was used to obtain the energies of dislocation cores, the results are consistent with ab initio calculations.

E.C. Do *et al.* [17] developed the MEAM potential (Modified Embedded-Atom Method) for gallium nitride, indium nitride and $Ga_{1-x}In_xN$ systems. The potential describes various physical properties (structural, elastic, defect properties) of a GaN crystal in good agreement with experimental data and calculations from the first principles.

These three potentials were tested on 15×15×15 nm^3 GaN supercell using three methods: melting simulation, elastic constants calculation, and track formation simulation for Xe ion with 167 MeV energy. The melting simulation test showed that all potentials give different melting point values (Fig. 5). The closest to the experimental value (2773 K) obtained by S. Porowski *et al.* [18] was achieved with MEAM potential. Elastic constants calculated with all three potentials are in good agreement with experimental data [19] (Table 2).

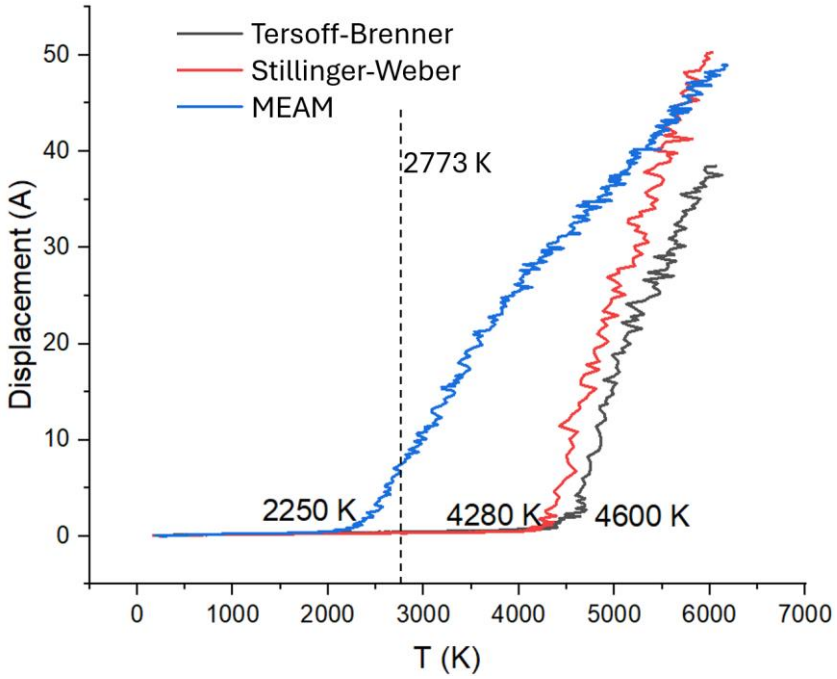

Figure 5. Dependence of the average atom displacement on the temperature in GaN.

Table 2. Comparison of experimental and calculated elastic constants.

	Elastic constants, GPa			
	Experiment	Tersoff-Brenner	Stillinger-Weber	MEAM
C_{11}	390±15	345	354	351

C_{12}	145±20	157	140	148
C_{13}	106±20	123	124	101
C_{33}	398±20	379	370	397
C_{44}	105±10	82	97	93

In track formation test a 100 ps simulation in LAMMPS program was performed using TREKIS data for Xe ion with 167 MeV energy. The track of Tersoff-Brenner potential has a 3.4 nm diameter which may differ depending on depth (Fig. 6a). The track of Stillinger-Weber potential was almost completely recrystallized (Fig. 6b). The track of MEAM potential has a 6.2 nm diameter, which appears to be too large (Fig. 6c). Therefore, it was decided to use the Tersoff-Brenner potential for further simulations with Pb ion. The results are discussed in the next section.

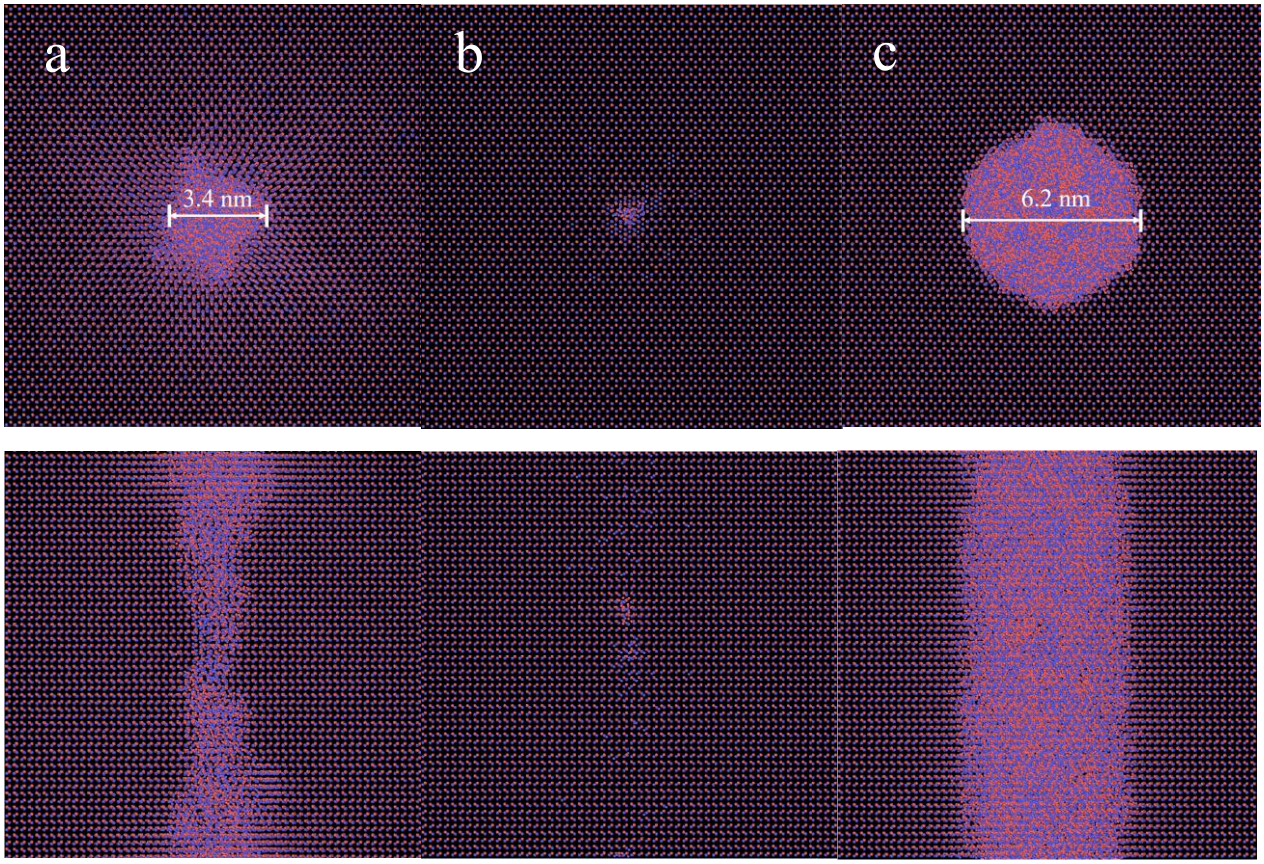

Figure 6. Top and side view of Xe ion tracks for Tersoff-Brenner (a), Stillinger-Weber (b) and MEAM (c) potentials at 100 ps.

3. Results and discussion

MD simulation of GaN lattice relaxation in SHI track was performed in LAMMPS program in 25×25×25 nm^3 supercell for Pb ion with 132 MeV energy.

Different crystallographic directions of the trajectory of the incoming ion were chosen ($[0,0,0,1], [1,\bar{1},0,0], [1,1,\bar{2},0]$), since S. Mansouri *et al.* [14] did not specify the ion direction in their work. But, according to the simulation results, the track structure depends on its orientation (Fig. 7).

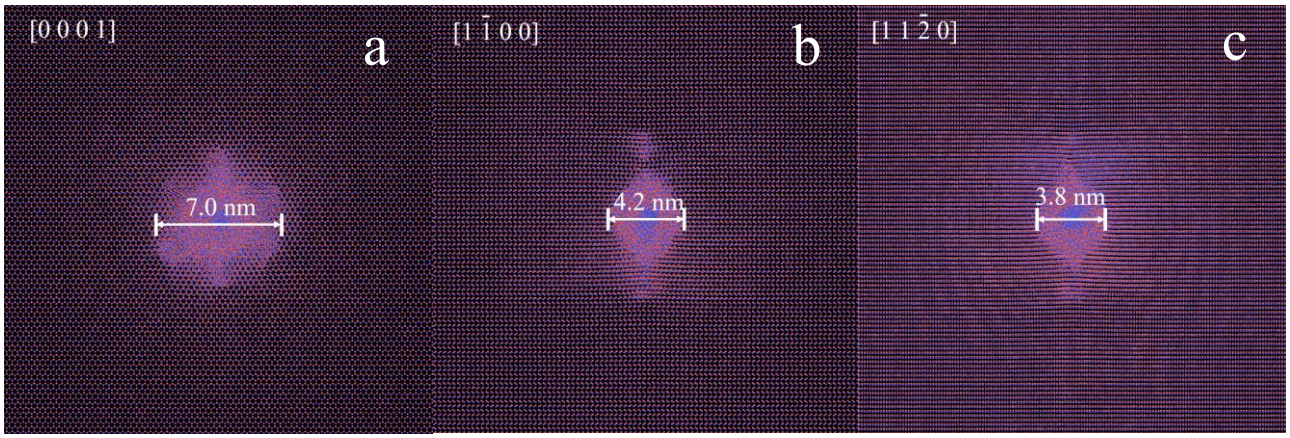

Figure 7. Track diameters for [0,0,0,1] (a), [1,-1,0,0] (b), and [1,1,-2,0] (c) directions at 200 ps.

The $[0,0,0,1]$ track appears to have a hexagonal form and a 7.0 nm diameter. But if we consider the cross sections of this track (width ~1 nm) at different depths, it becomes clear that the track has a round shape and diameter of ~3.6 nm (Fig. 8), which corresponds to the experimental value of 3nm from [14]. And around this track lattice deformations appear in certain directions, which create hexagonal form by overlapping. The $[1,\bar{1},0,0]$ and $[1,1,\bar{2},0]$ tracks have similar forms and diameters of 4.2 nm and 3.8 nm respectively. By inspecting cross sections of these tracks (width ~ one atomic layer) the curvature of atomic planes and extra planes can be seen on opposite sides of these tracks (Fig. 9). By overlapping, these deformations create structures in (Fig. 7). So, it seems that tracks relaxation and recrystallization do not occur uniformly. There are certain directions along which recrystallization is weaker. Deformations in material can extend beyond track diameter and may affect material strength or its other properties.

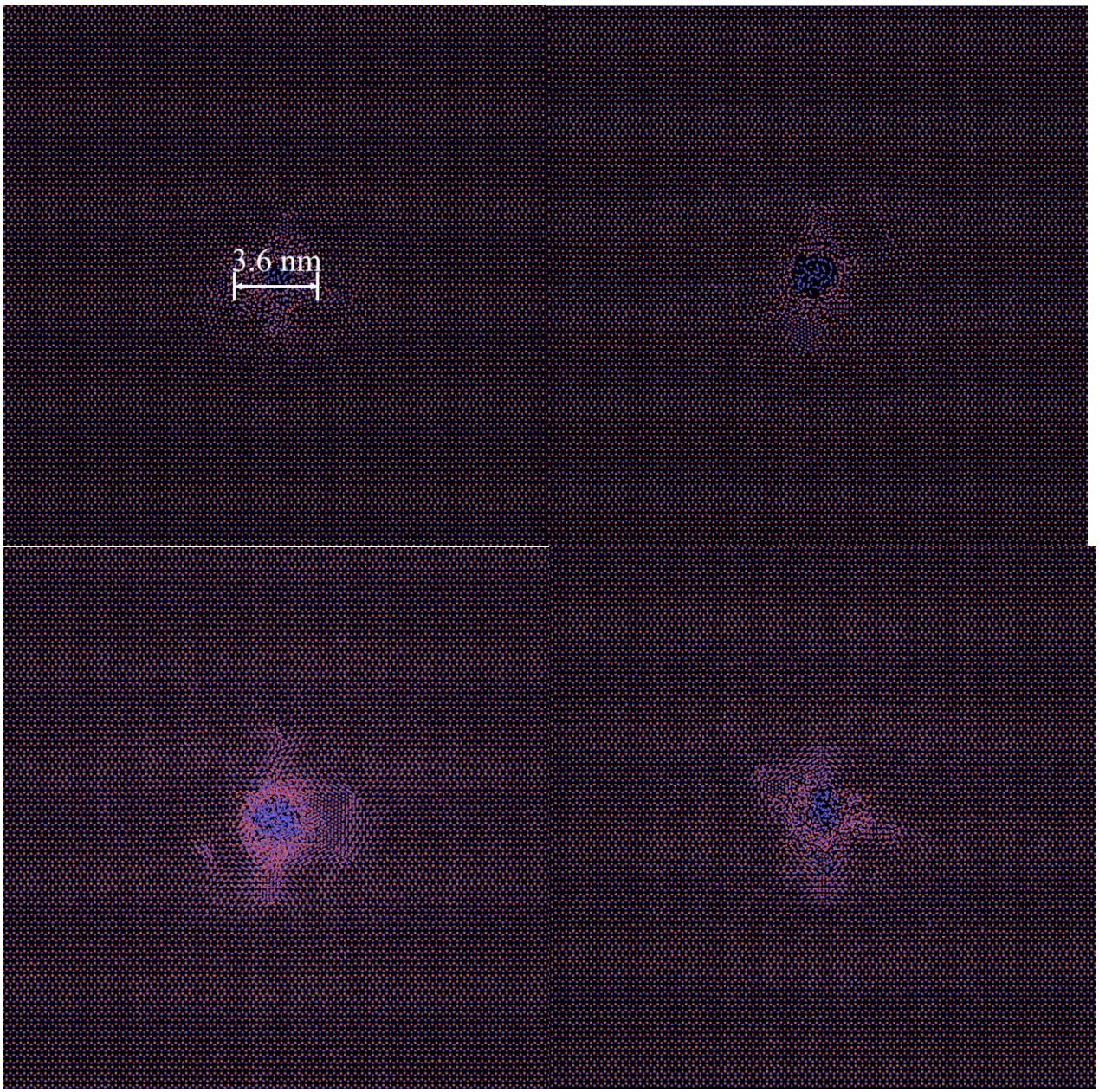

Figure 8. Cross sections of [0,0,0,1] track on different depths.

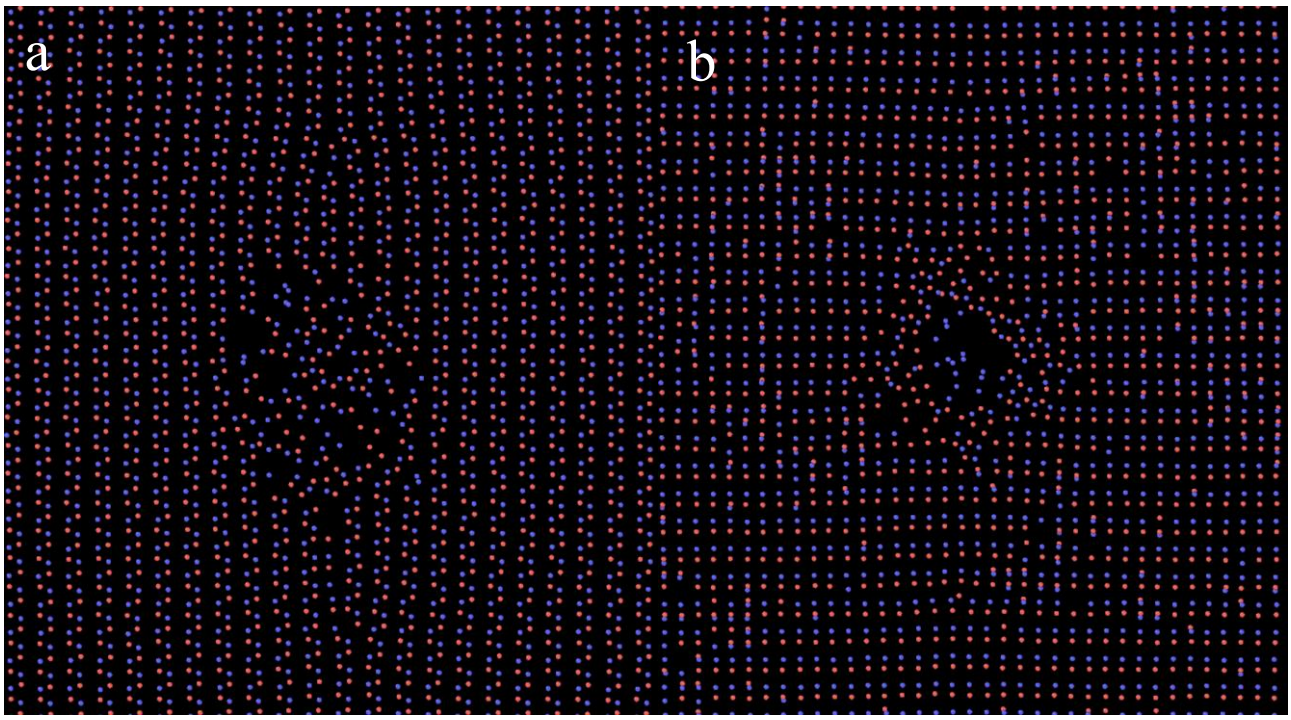

Figure 9. Monoatomic cross sections of [1,-1,0,0] (a) and [1,1,-2,0] (b) tracks.

Conclusion

A simulation of SHI effects in α-GaN was performed by combining Monte-Carlo and molecular dynamics methods in TREKIS and LAMMPS programs. For that purpose, the energy loss function was constructed, and the most suitable interatomic potential for SHI track formation description was found – Tersoff-Brenner potential.

The structural transformations of crystal lattice were investigated. Tracks have different diameters – 3.6, 4.2, 3.8 nm – and different forms depending on orientation of incoming SHI trajectory relative to the crystal lattice. The damage caused to the material consists not only of the track, but also of lattice deformations outside the track.

For verification of these results additional experiments on SHI passing through GaN in certain directions need to be conducted.

References

[1] S. Taranovich, "GaN in Space," *Power Syst. Des.*, 2019.

[2] N. A. Medvedev, R. A. Rymzhanov, and A. E. Volkov, "Time-resolved electron kinetics in swift heavy ion irradiated solids," *J. Phys. D. Appl. Phys.*, vol. 48, no. 35, p. 355303, Aug. 2015, doi: 10.1088/0022-3727/48/35/355303.

[3] A. P. Thompson *et al.*, "LAMMPS - a flexible simulation tool for particle-based materials modeling at the atomic, meso, and continuum scales," *Comput. Phys. Commun.*, vol. 271, p. 108171, Feb. 2022, doi: 10.1016/J.CPC.2021.108171.

[4] L. Van Hove, "Correlations in Space and Time and Born Approximation Scattering in Systems of Interacting Particles," *Phys. Rev.*, vol. 95, no. 1, p. 249, Jul. 1954, doi: 10.1103/PhysRev.95.249.

[5] S. Adachi, "Optical Constants of Crystalline and Amorphous Semiconductors," *Opt. Constants Cryst. Amorph. Semicond.*, 1999, doi: 10.1007/978-1-4615-5247-5.

[6] H. Sobotta, H. Neumann, R. Franzheld, and W. Seifert, "Infrared lattice vibrations of GaN," *Phys. status solidi*, vol. 174, no. 2, pp. K57–K60, 1992, doi: 10.1002/PSSB.2221740231.

[7] S. Logothetidis, J. Petalas, M. Cardona, and T. D. Moustakas, "Optical properties and temperature dependence of the interband transitions of cubic and hexagonal GaN," *Phys. Rev. B*, vol. 50, no. 24, p. 18017, Dec. 1994, doi: 10.1103/PhysRevB.50.18017.

[8] C. G. Olson, D. W. Lynch, and A. Zehe, "10-30-eV optical properties of GaN," *Phys. Rev. B*, vol. 24, no. 8, p. 4629, Oct. 1981, doi: 10.1103/PhysRevB.24.4629.

[9] B. L. Henke, E. M. Gullikson, and J. C. Davis, "X-Ray Interactions: Photoabsorption, Scattering, Transmission, and Reflection at E = 50-30,000 eV, Z = 1-92," *At. Data Nucl. Data Tables*, vol. 54, no. 2, pp. 181–342, Jul. 1993, doi: 10.1006/ADND.1993.1013.

[10] R. H. Ritchie and A. Howie, "Electron excitation and the optical potential in electron microscopy," *Philos. Mag.*, vol. 36, no. 2, pp. 463–481, 1977, doi:

10.1080/14786437708244948.

[11] A. Akkerman, T. Boutboul, A. Breskin, R. Chechik, A. Gibrekhterman, and Y. Lifshitz, “Inelastic electron interactions in the energy range 50 eV to 10 keV in insulators: Alkali halides and metal oxides,” *Phys. Status Solidi B-Basic Res.*, vol. 198, no. 2, pp. 769–784, 1996, doi: 10.1002/PSSB.2221980222.

[12] H. Nikjoo, S. Uehara, and D. Emfietzoglou, “Interaction of Radiation with Matter,” *Interact. Radiat. with Matter*, pp. 1–343, Jan. 2016, doi: 10.1201/B12109/INTERACTION-RADIATION-MATTER-HOOSHANG-NIKJOO-SHUZO-UEHARA-DIMITRIS-EMFIETZOGLOU.

[13] J. F. Ziegler and J. P. Biersack, “The Stopping and Range of Ions in Matter,” *Treatise Heavy-Ion Sci.*, pp. 93–129, 1985, doi: 10.1007/978-1-4615-8103-1_3.

[14] S. Mansouri *et al.*, “Swift heavy ion effects in gallium nitride,” *Int. J. Nanoelectron. Mater.*, vol. 1, no. January, pp. 101–106, 2008.

[15] J. Nord, K. Albe, P. Erhart, and K. Nordlund, “Modelling of compound semiconductors: Analytical bond-order potential for gallium, nitrogen and gallium nitride,” *J. Phys. Condens. Matter*, vol. 15, no. 32, pp. 5649–5662, Aug. 2003, doi: 10.1088/0953-8984/15/32/324.

[16] A. Béré and A. Serra, “On the atomic structures, mobility and interactions of extended defects in GaN: Dislocations, tilt and twin boundaries,” *Philos. Mag.*, vol. 86, no. 15, pp. 2159–2192, May 2006, doi: 10.1080/14786430600640486.

[17] E. C. Do, Y. H. Shin, and B. J. Lee, “Atomistic modeling of III-V nitrides: Modified embedded-atom method interatomic potentials for GaN, InN and Ga1-xInxN,” *J. Phys. Condens. Matter*, vol. 21, no. 32, 2009, doi: 10.1088/0953-8984/21/32/325801.

[18] S. Porowski *et al.*, “The challenge of decomposition and melting of gallium nitride under high pressure and high temperature,” *J. Phys. Chem. Solids*, vol. 85, pp. 138–143, Oct. 2015, doi: 10.1016/J.JPCS.2015.05.006.

[19] A. Polian, M. Grimsditch, I. Grzegory, A. Polian, M. Grimsditch, and I. Grzegory, “Elastic constants of gallium nitride,” *JAP*, vol. 79, no. 6, pp. 3343–3344, Mar. 1996, doi: 10.1063/1.361236.